II. Articles

Chapter 1 Examination of Restoration Methods for the South Sanctuary of Western Prasat Top

Taisei Geotech Mituharu FUKUDA

Section 1 .Structure and Foundation of the South Sanctuary of West Prasat Top

Among the West Prasat Top remains, the South Sanctuary shall be restored first. The South Sanctuary is composed of an upper foundation and lower platform as shown in Fig. 2, and a main sandstone structure on the upper foundation as shown in Photo 1. The original soil below the lower platform digs into the natural ground at depths below N22, and is composed of three-tiered sandstone side walls and stone lines below the walls, which further dig into the ground to a depth of approximately 80cm. The sandstone side walls of the lower platform stops immediately above the stone lines, below which is a bare hole with no sandstone walls.

The main sandstone structure distributes its load from the stones that pave the central level to the soil inside the foundation. As shown in the diagram of the side structure (Fig. 2), the sandstone side walls of the upper and lower platforms are arranged around the perimeter of the main sandstone structure, and do not directly receive the load of the main structure. Additionally, the side walls of the lower platform are positioned outside the width of the side walls of the upper foundation, so the loads of the two side walls do not overlap. The two tiers of side walls are thus supported by the foundation and natural ground beneath the walls.

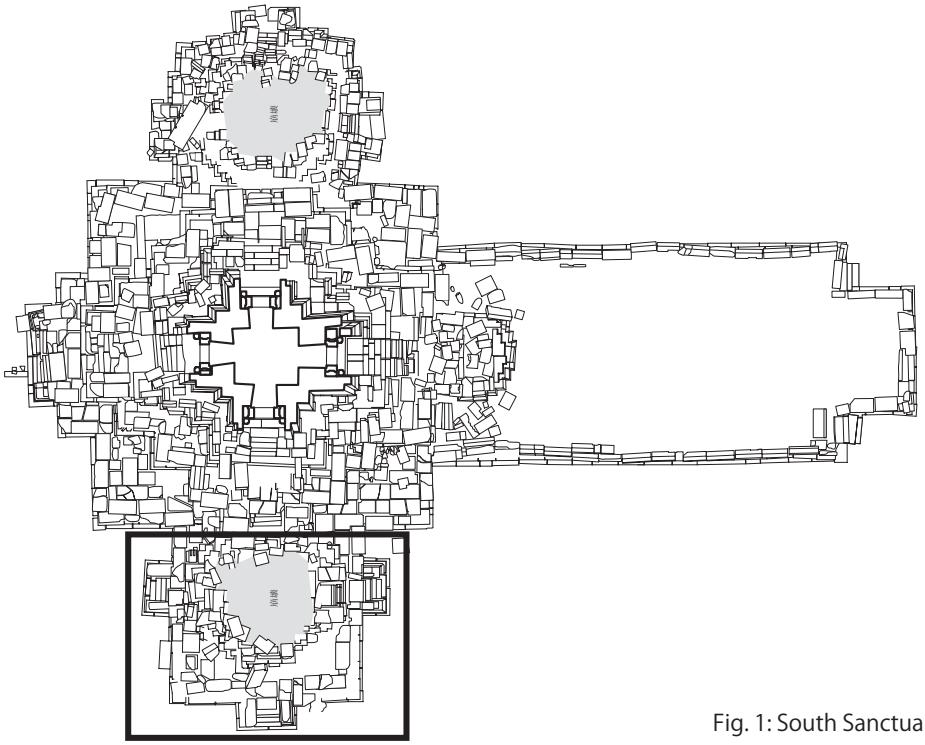

Fig. 1: South Sanctuary of West Prasat Top

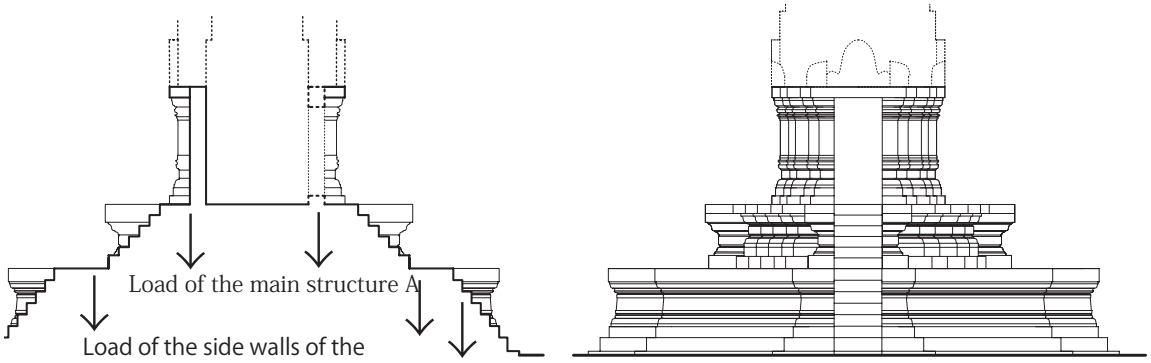

Fig. 2: Structure of the South Sanctuary

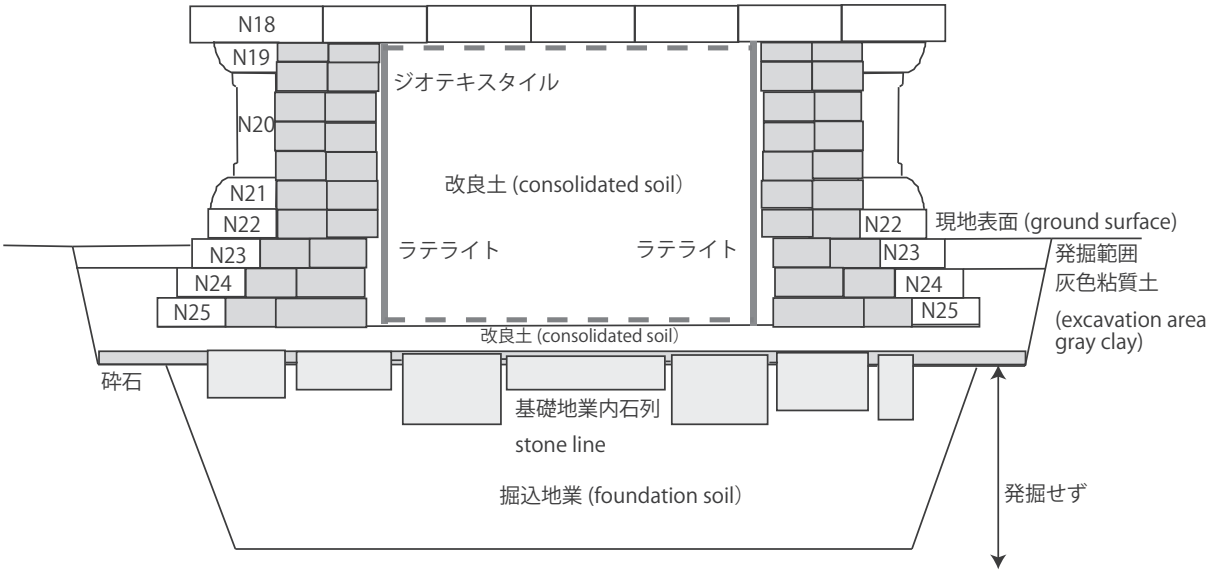

Fig. 3: Structure of the lower platform

Photo 1: Temporary assembly of the main structure of the South Sanctuary

2. Deformation of the South Sanctuary of West Prasat Top

Photos 2 and 3 show the South Sanctuary viewed from the east. On the whole, no major deformation is seen in the height level of the lower platform. The main structure is tilted from the north to the south side, and the upper foundation is also tilted from the north side of the main structure to the south side as though in response to the tilting of the main structure. However, the upper foundation practically maintains a level height from the north side of the South Sanctuary to the north side. There is no major bulging in the east face of the upper foundation, and the tilting is predominantly seen in the north-south direction.

Photo 4 shows subsidence of the upper foundation, and Photo 5 shows subsidence of the central area of the sandstone pavement of the surface of the lower platform. Measured from the sandstone side walls on both sides, it is sunken approximately 56cm at the most. However, the subsidence is minimal on the north side, which connects with the Central Sanctuary. Since it has been found in an excavation survey that the south stairways of the Central

Sanctuary have not shifted from its original position, the subsidence is most predominantly observed at the base of the South Sanctuary. The lower platform displays sandstone side walls that are level on the whole, but local subsidence is especially conspicuous in the center.

Photo 6 shows the stone lines below the lower platform. As the natural ground exists approximately 80cm below these lines, the foundation material fills the 80-centimeter space below the stone lines. Irregular-shaped flat sandstone is divided by the stone lines, but no evident signs of subsidence can be observed. The south stairways of the Central Sanctuary to the north of the stone lines basically maintain a level height. Thus, it is clear that the foundation material has subsided on the south side of the south stairways of the Central Sanctuary, from the upper and lower platforms above the natural ground, and that this subsidence is the direct cause of the deformation of the South Sanctuary.

Photo 2: The Central Sanctuary and South Sanctuary viewed from the east

Photo 3: South Sanctuary viewed from the east

Photo 4: Subsidence of the top surface of the upper foundation

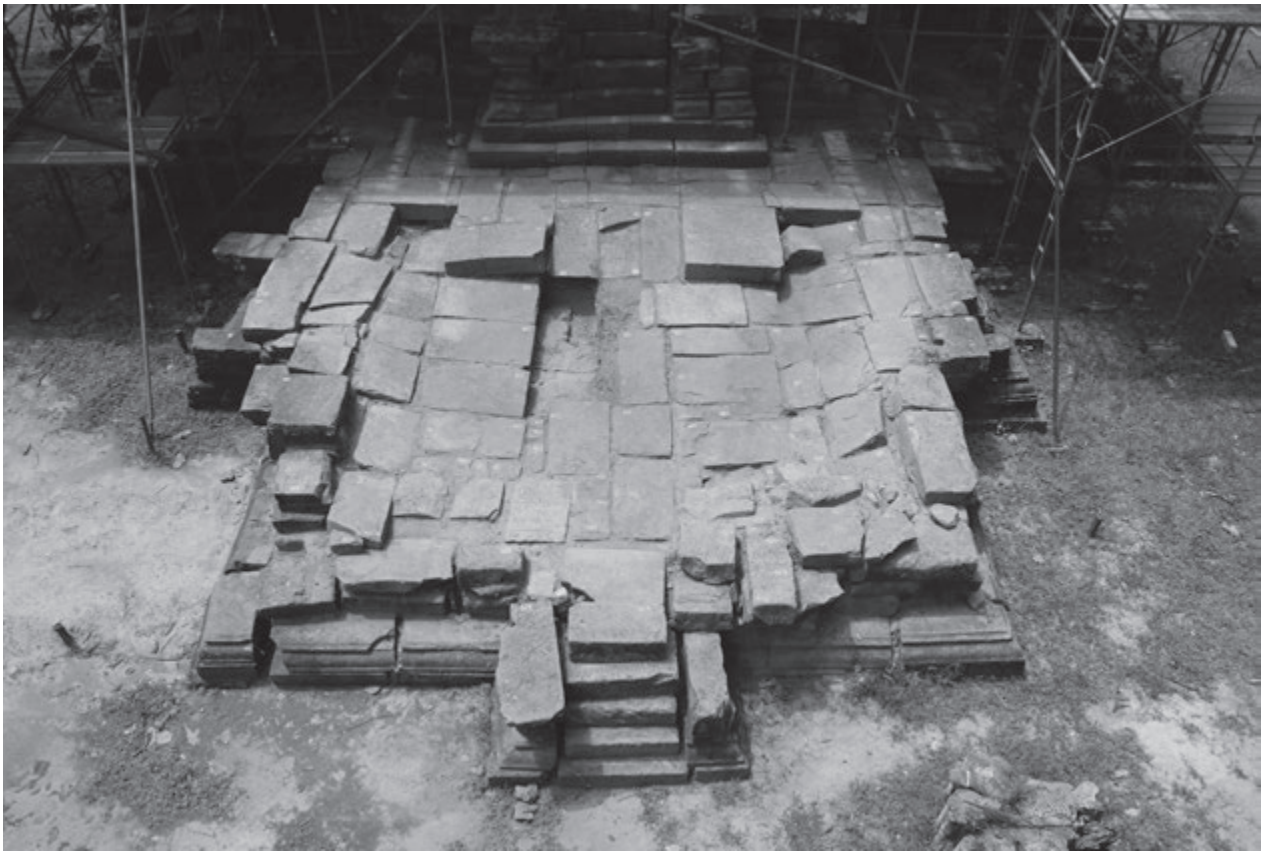

Photo 5: Subsidence of the paving stones on the surface of the lower platform

Photo 6: Stone lines directly beneath the lower platform

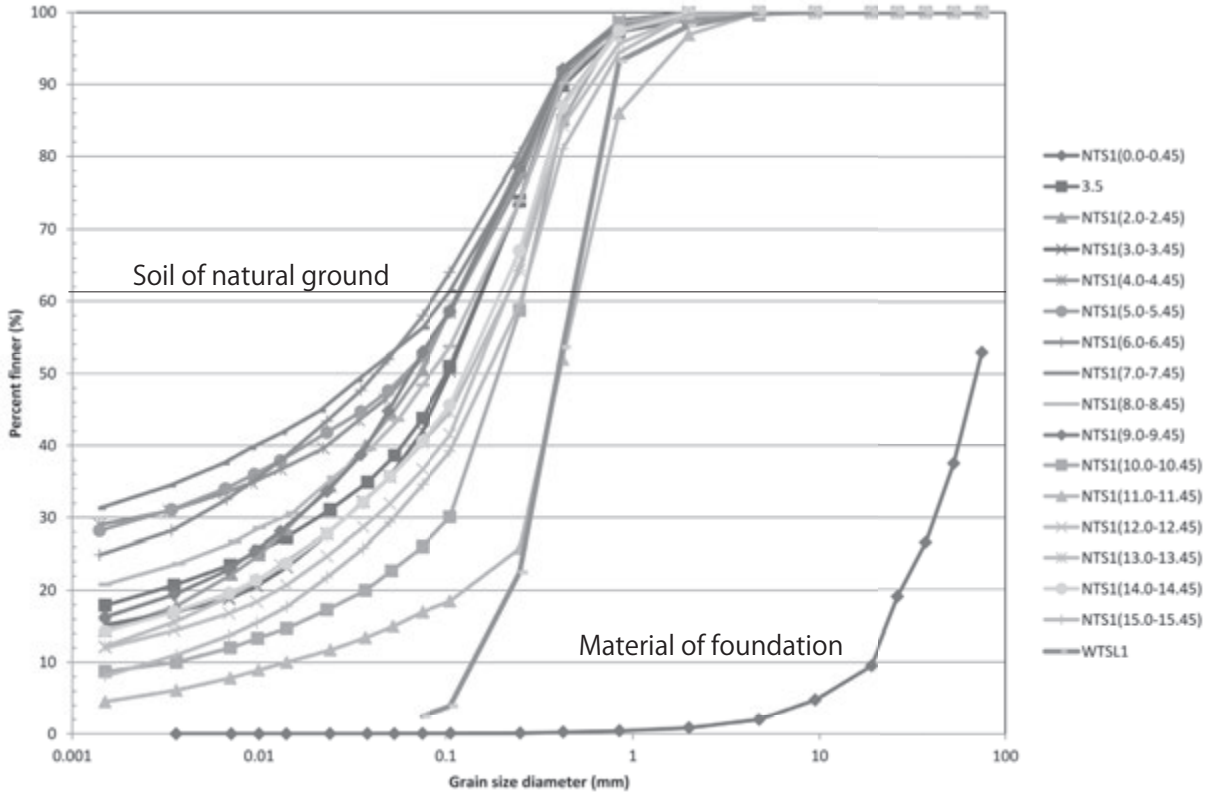

Fig. 4: Grain size distribution of the foundation material at the South Sanctuary

3. Foundation Material and Degree of Compaction

The foundation material is coarse sand with readily erodible properties. The solid line in Fig. 4 represents the grain size distribution of the foundation material. The dotted lines show the grain size distribution of sample soils collected from a natural ground boring survey conducted at Western Prasat Top. The foundation material is composed mostly of coarse grains that are more than 0.1mm in diameter. Contrarily, soils from the natural ground are composed mostly of fine grains.

As the grain size characteristics are not readily apparent by the above graph alone, the grain size distribution curves shall be expressed in terms of a representative index, although details will be omitted. That is, in terms of representative diameter, a diameter index of 10-2mm or more expresses the property of sand, 10-3 to 10-2mm the property of silt, and 10-3mm or less the property of clay. Fig. 5 shows an overview of the representative diameter index. The representative diameter index of the natural ground, according to the figure, is (1 to 2) × 10-2mm in the surface layer and lower layers, which indicates sand layers, and ranges between (3 to 7) × 10-3mm in the intermediate layers, which indicate silt layers. Meanwhile, the representative diameter index of the foundation material is 1.1 × 10-1mm, which represents sand, and indicates that the foundation material is made of coarser sand compared to the sand layers of the natural ground.

Fig. 6 shows the relationship between representative diameter index and soil properties. In this figure, liquefaction refers to the runoff of sand accompanying the runoff of water from the ground surface caused by a rise in the pore pressure of sand layers due to an earthquake. In other words, sand that is susceptible to liquefaction has properties that make it easy for it to run off along with the runoff of water. Photo 7 shows a ground subsidence that occurred due to liquefaction and the runoff of sand in Urayasu in the wake of the Great East Japan Earthquake of March 11, 2011. The ground around the building, which is supported by piles, had subsided, making the concrete foundation appear as though it is floating.

The representative diameter index of soils susceptible to liquefaction ranges from 2 × 10-2mm to 5 × 10-1mm. Thus, while the sand layers of the natural ground do not fall within the scope of liquefaction, as they contain rather fine grains, the foundation material has properties that make it susceptible to liquefaction. It can thus be assumed that the sand in the foundation material has properties that make it susceptible to runoff accompanying the runoff of water.

Photo 8 shows the bare hole of a permeability test performed on the lower platform. The hole maintained its shape in wet condition, but when water was quietly applied, the area around the hole eroded as though to melt, and the hole lost its shape.

Photo 9 shows a state of compaction by watering. After a loading test was performed in wet condition, sprinkling water around the load plate caused immediate subsidence, or collapse, of the soil.

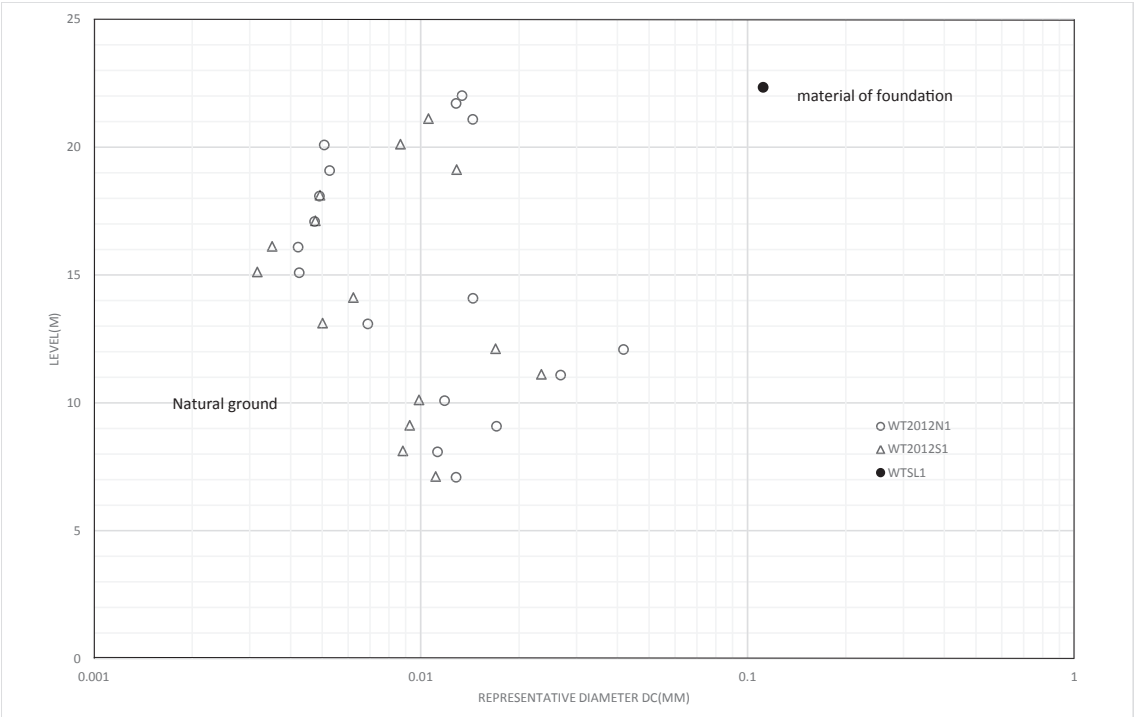

Fig. 5: Grain size properties of the natural ground and foundation material

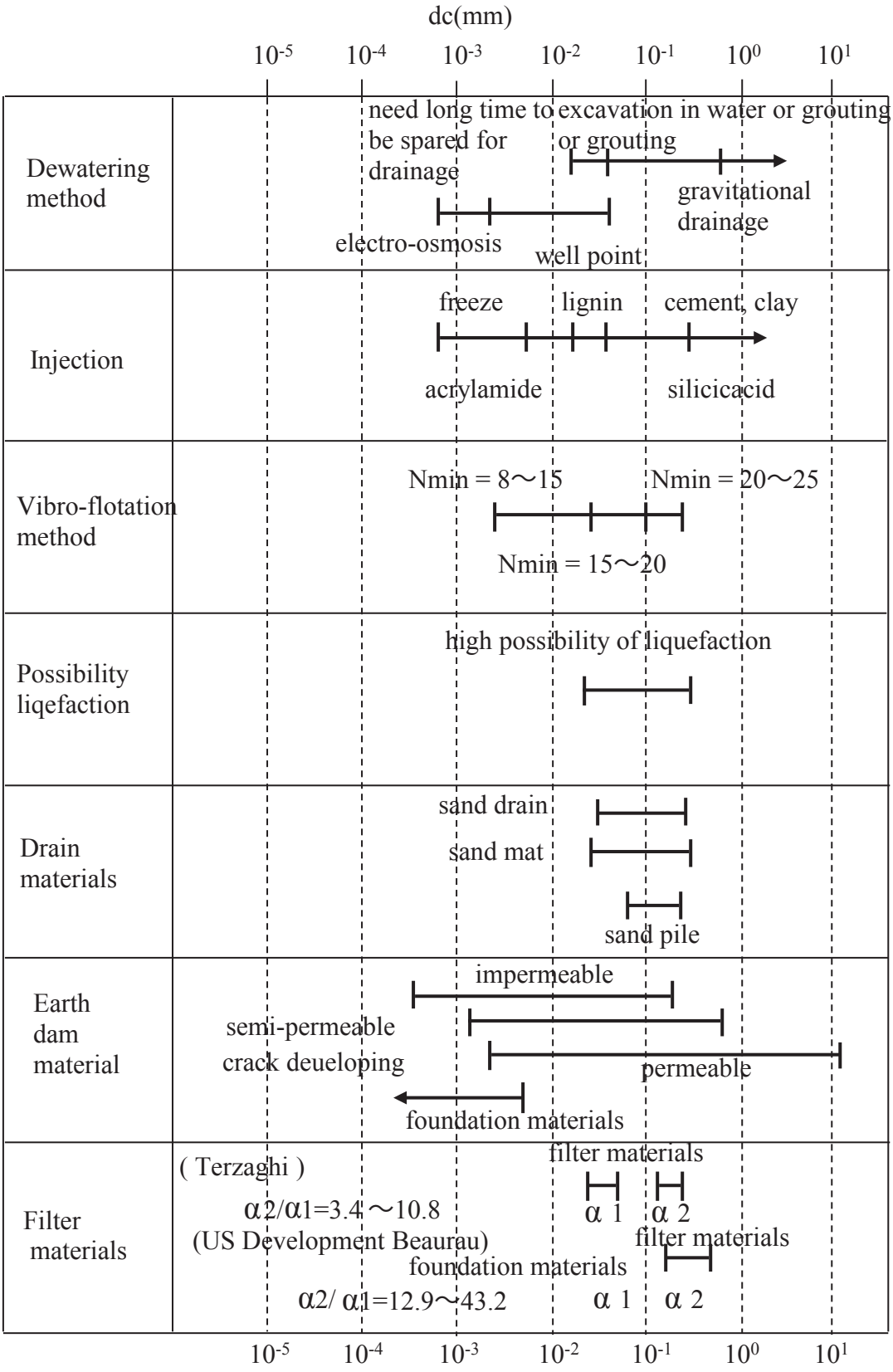

Fig. 6: Representative diameters and soil properties

Photo 7: Ground subsidence caused by liquefaction in Urayasu in the wake of the Great East Japan Earthquake

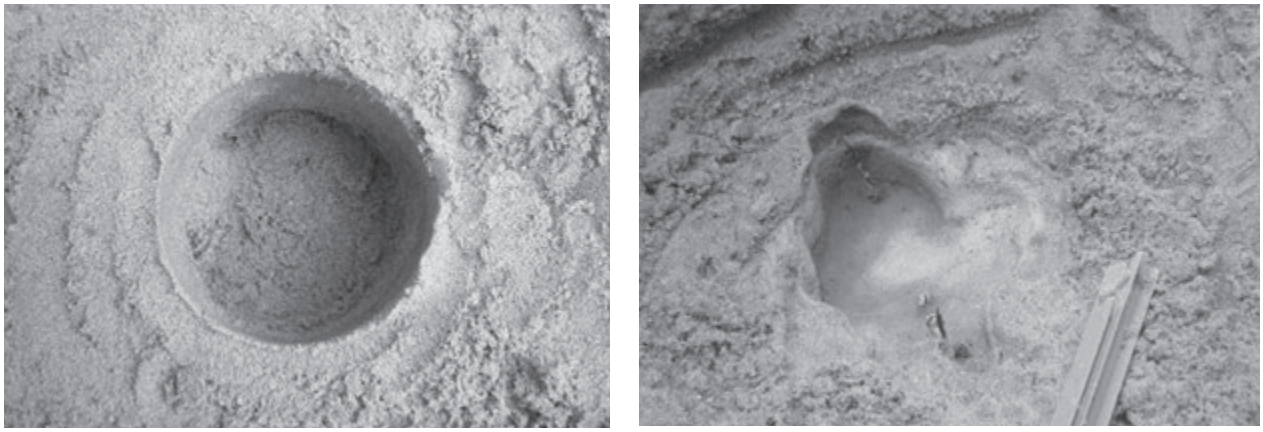

Photo 8: Erosion of the material of the lower platform

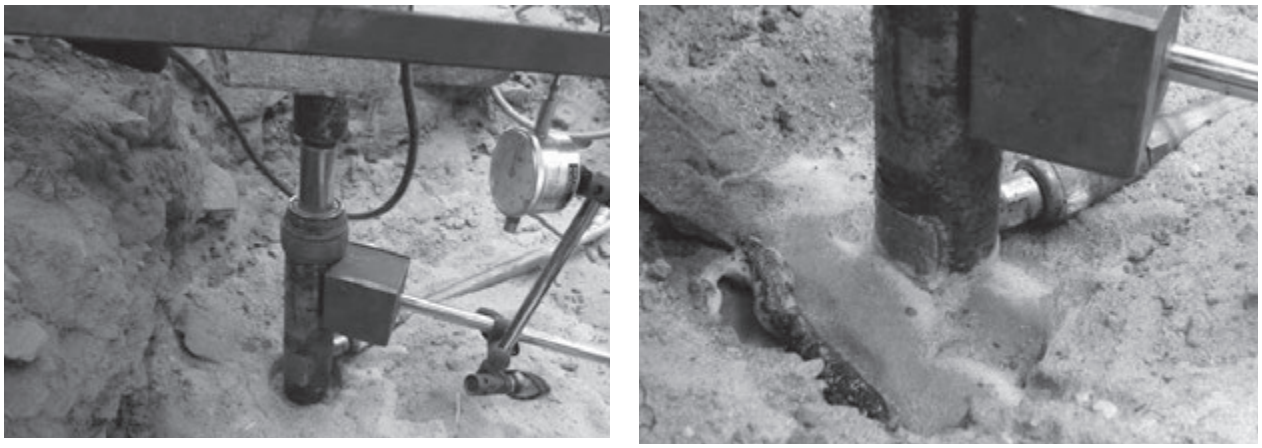

Photo 9: Water sprinkling around the load plate in a loading test

The possibility of a material that is susceptible to liquefaction actually liquefying is reduced if it is thoroughly compacted and solidified. To examine this theory, a penetration test was performed. Fig. 7 shows N values. The N value of the lower platform is less than 5, and the N value of the soil below the stone lines is between 5 and 10. There is thus a clear difference in density between the soil material of the lower platform and the soil below the stone lines. Table 1 shows a classification of density based on N values by Terzaghi and Peck. According to this table, the N value of the surface layer corresponds to “very loose” density, and the soil below the stone lines is classified as having “loose” density. Again, there is a clear difference between the material of the lower platform and the soil below the stone lines, with the soil below the stone lines being more compacted compared to the soil above it.

The figure also shows the N values of the natural ground. As a whole, it has an N value of over 10. A grain size test showed that it contains a rather large amount of fine grains compared to the sand of the foundation material, so a simple comparison cannot be made, but it is more solid than the material of the lower platform.

The loose foundation material can be confirmed by the results of an onsite density test. Table 2 shows the results of the test. The foundation material has a dry density of less than 1.5g/cm3, and is thus loose. Loose density and coarse sand can be expected to deliver only low bearing power and a high coefficient of permeability.

Fig. 8 shows the result of a loading test performed on the lower platform. Ultimate bearing capacity is approximately 340kN/m2, and much smaller than that of the soil materials of the Angkor Monuments. Fig. 9 shows the result of an onsite permeability test. The coefficient of permeability of the loose and coarse sand of the lower platform is 1 × 10-1cm/s, but that of the rather solidified soil below the stone lines is 2 × 10-2cm/s and one order lower.

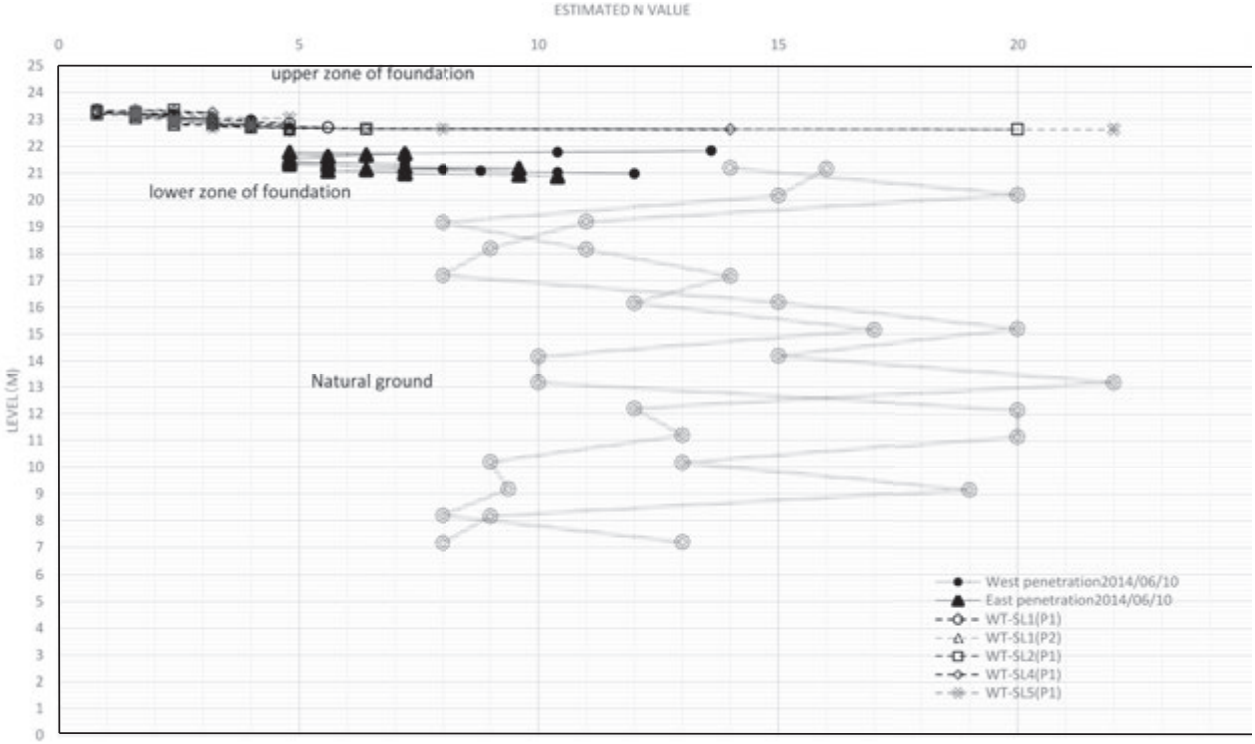

Fig. 7: N values

N value	Relative density by Terzaghi and Peck
0 ～ 4	very loose
4 ～ 10	loose
10 ～ 30	medium
30 ～ 50	dense
>50	very dense

Table 1: Relative density by Terzaghi and Peck

WTSL				
Location	Density method	Wet density (g/cm3)	Water content (%)	Dry density (g/cm3)
WTSL3(D1)	Sand replacement	1.68	4.94	1.60
WTSL2(D1)	Ring	1.43	2.03	1.40
WTSL1(D1)	Ring	1.54	2.94	1.50
WTSL5(D1)	Ring	1.49	2.76	1.45
WTSL5(D2)	Ring	1.46	2.86	1.42
Average		1.52	3.10	1.47

Table 2: Density of the lower platform of the South Sanctuary of West Prasat Top

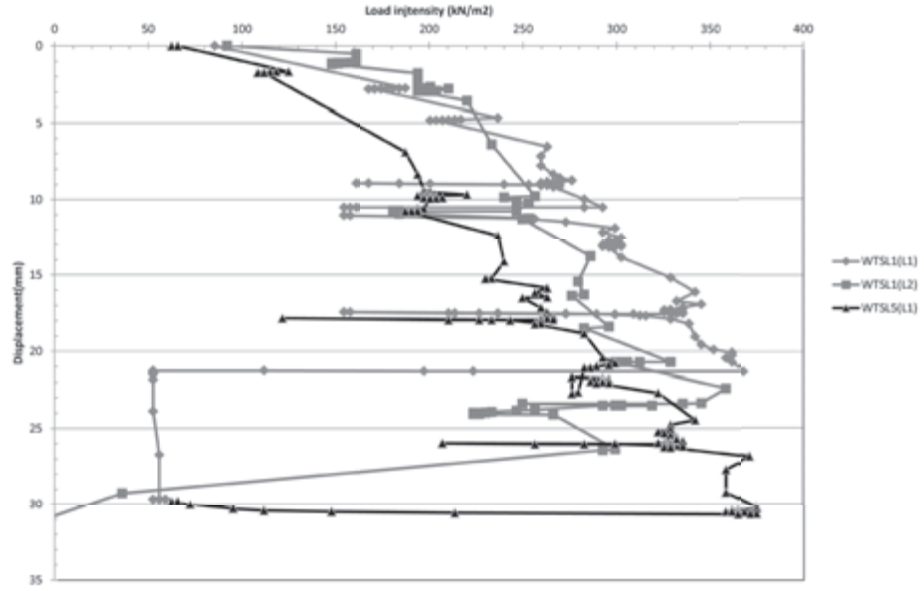

Fig. 8: Loading test result

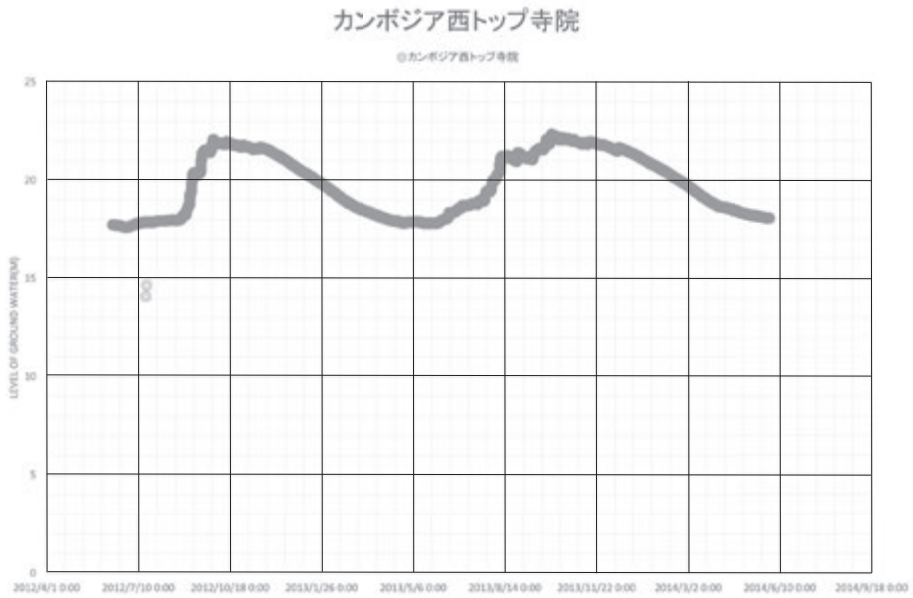

Fig. 9: Annual changes in groundwater level

The figure also shows the coefficient of permeability of consolidated soils used as test soils, as will be discussed later. The coefficient of permeability of test soil A is 2×10^{-3}cm/s, and that of test soil B is approximately 2×10^{-2}cm/s.

Judging by samples collected in a hand auger test, the material of the lower platform and the soil below the stone lines have the same soil qualities, and are both composed of coarse sand. However, the two layers are classified differently based on their N value and coefficient of permeability, and the soil below the stone lines is estimated as having higher density. It needs to be examined why two soil materials that have the same qualities and are both found in a foundation have such different properties.

Fig. 10 shows changes in the level of groundwater in the natural ground over a period of two years. It shows that it reached approximately 22m at the highest during the rainy season. Since the stone lines are found at a height of roughly 22m, the soil below the stone lines went below and above the groundwater level at different times and was naturally compacted by watering. This change in groundwater level might also be an effective factor in the consolidation of the soil below the stone lines.

4. Required Bearing Capacity at the South Sanctuary

The fact that the deformation of the South Sanctuary of West Prasat Top is mainly a result accompanying the runoff of sand caused by gully erosion of the foundation material has so far been documented. However, the erosion is a runoff that occurs due to the material being loose, coarse sand. The condition of loose, coarse sand can also be assessed by its low-intensity bearing capacity. Thus, consolidation of the foundation material plays an important role in the restoration of the South Temple.

As shown in Fig. 2, the maximum load of the South Temple is the load of the main structure that bears upon the upper foundation. The loads of the side walls of the upper foundation and side walls of the lower platform are respectively transmitted vertically downward, but these loads are small. Therefore, it suffices for the foundation material to have enough bearing capacity to safely support the load of the main structure of the South Temple. However, as the final appearance of the South Temple has not yet been clarified, the load was calculated as shown in Table 3 by scaling up the appearance of the Central Temple and estimating a larger load than reality. The required maximum ultimate bearing capacity was calculated as approximately 200kN/$m^2$to 300kN/m^2However, when assuming a safety factor of 3 to safely secure this bearing capacity, an ultimate bearing capacity of approximately 900kN/m^2 is required.

Compared to this 900kN/m^2 required maximum ultimate bearing capacity, the 340kN/m^2 ultimate bearing capacity obtained in the loading test performed on the lower platform is extremely small, and can be evaluated as having a bearing capacity with a safety factor of 1 or so. Thus, it is clear that the bearing capacity of the foundation material must be significantly improved compared to its present strength. A large bearing capacity would also lead to stronger resistance against gully erosion.

Scale	Drawing (cm)	Scale	Length (m)	Mass (kN)	Max. load strength (kN/m2)
Present height	8.7	100	8.7	197.0	197.0
Restored height	9.6	150	14.4	326.1	326.1
Upper tier width	10.2	100	10.2		
Lower tier width	19.1	100	19.1		
Present height from top tier	6.3	100	6.3	142.7	
Restored height from top tier	7.5	150	11.25	254.8	
Wet density (kN/m3)	22.6				

Table 3: Design requirement of ultimate bearing capacity

5. Consolidation and Authenticity of the Restored Soil Material

The basic principle for securing authenticity in the preservation of monuments is to reutilize the materials that have been excavated and to restore the monuments to their initial appearance. However, the original foundation material at the South Temple is coarse sand with loose density, which makes it susceptible to gully erosion and subsidence caused by the load of the main structure. Therefore, it is impossible to restore the temple with the soil in the loose condition that was found at the time of dismantlement.

A possible method for securing bearing capacity and preventing gully erosion was to provide support by inserting a concrete box culvert-like structure inside the foundation, but this would not necessarily adhere to the authenticity of preservation. A measure was thus sought to slightly improve the coarse sand excavated from the foundation and apply it to the restored foundation. If the foundation material could be improved by making a slight improvement to the sand, authenticity could be protected. Therefore, a measure was ultimately taken to strengthen gully erosion resistance by mixing a small amount of clay to the coarse sand that was excavated and promote grain cohesion by mixing slaked lime and laterite powder, and thereby improving erosion resistance and enhancing bearing capacity.

Another possible method was to try to prevent soil runoff using geotextile instead of improving the coarse excavated sand, but as coarse sand is difficult to compact, sufficient bearing capacity cannot be expected. It was also conceivable to use geotextile to reinforce bearing capacity, but restoring the foundation using coarse sand that is susceptible to gully erosion would leave cause for concern. For this reason, it was reasonable to first consider improving the coarse sand.

Fig. 10 shows the result of a compaction test. The solid lines represent the relationship between water content and dry

density. The dotted lines are the result of a Yamanaka hardness test that was performed to examine the strength property of the compacted soil, and represent the relationship between water content and the Yamanaka hardness index. The ● symbol in the figure represents the coarse excavated sand. The compaction curve does not show a clear peak, and remains flat. This means that the material is difficult to compact. The compaction curve becomes convex when clay is mixed at a ratio of 1 and 0.3 to the volume of the coarse sand, and optimal compaction condition changes according to the material. At the same time, the Yamanaka hardness index also becomes convex, and strength also increases. Fig 11 shows this change in the form of grain size distribution curves.

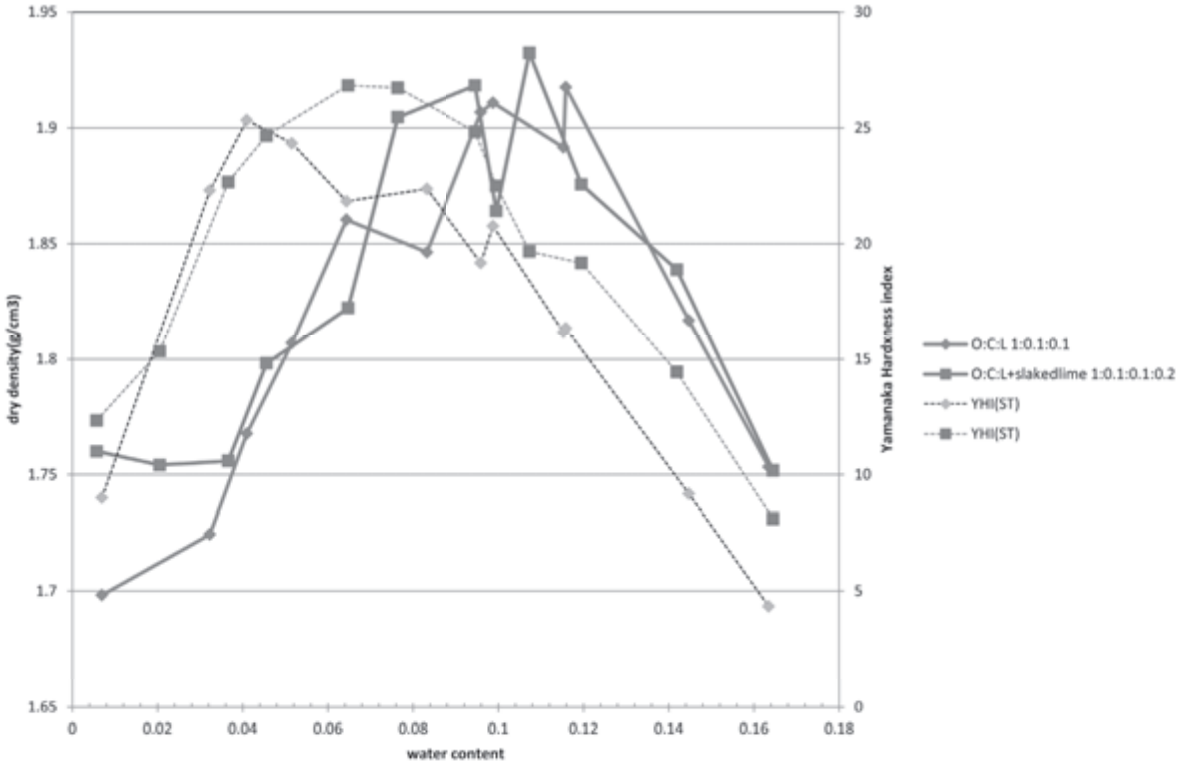

Fig. 10: Compaction test

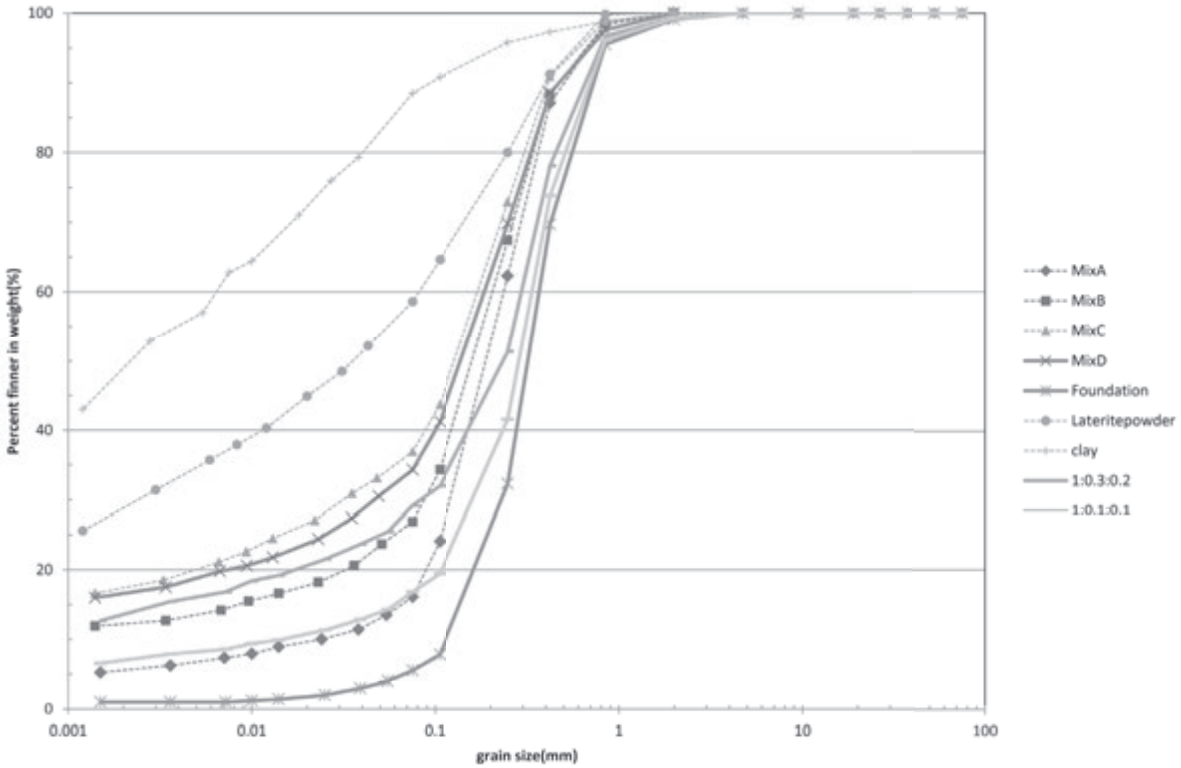

Fig. 11: Consolidation of the excavated soil

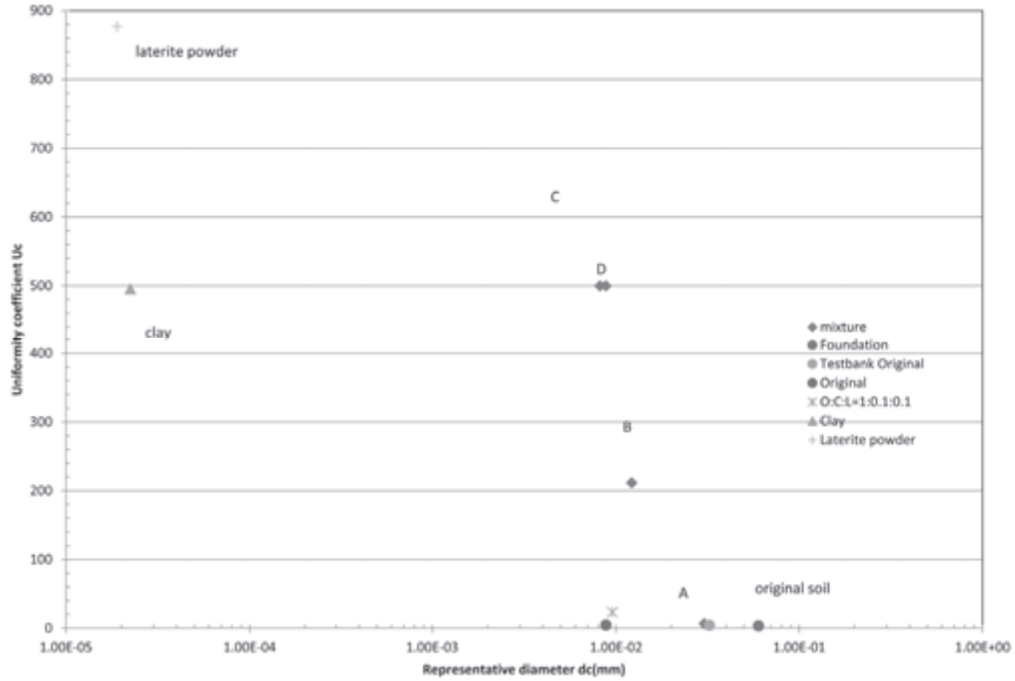

Fig. 12 : Consolidation of the coarse excavated sand by mixing clay

Fig. 12 shows that the foundation material is composed of coarse sand. It also shows the grain size distribution curves when clay and laterite powder are respectively mixed with the coarse sand. Laterite power is expected to provide cohesion between clay particles. The grain size distribution curves of the two mixtures are shown below.

Original : clay : laterite powder = 1 : 0.3 : 0.2

Original : clay : laterite powder = 1 : 0.1 : 0.1

MixA to MixD in the figure are grain size distribution curves showing mixture effects accumulated in the restoration of the Angkor Monuments. It is clear that soil mixture (A) is similar to MixB, and soil mixture (B) is similar to MixA.

The excavated soil used in the compaction test was mixed with a small amount of fine particles with a representative diameter of 6×10^{-2}mm, as shown in Fig 12. The representative diameter of the clay to be mixed with the excavated soil is 2×10^{-5}mm, and that of laterite powder is also 2×10^{-5}mm. Based on this, the representative diameter of soil mixture (B) above becomes 1×10^{-2}mm. Compared to the range of liquefaction shown in Fig. 6, the excavated soil falls within the range of liquefaction, but soil mixture (B) falls outside it, and shows that erosion resistance has been reinforced.

6. Confirmation of Bearing Capacity and Erosion Resistance of Test Soils

Test foundations were created to confirm the quality of soils that are consolidated by mixing clay and laterite powder to the coarse excavated sand. The main objectives were to confirm the mechanical features of the soil mixtures, and to accumulate experience in people who engage in foundation work. The blending ratio and test conditions are shown below. The grain size distribution curve of test soil B is shown in Fig. 13.

Test soil A Excavated soil : clay : laterite powder = 1 : 0.1 : 0.1

Test soil B Excavated soil : clay : laterite powder : slaked lime = 1 : 0.1 : 0.1 : 0.2

Compaction was performed using a rammer called “elephant’s foot” and a round rammer. Photos 10 to 27 show the progress of the test foundation work. In Photo 10, large rubbles and foreign matters contained in the excavated soil were removed and sifted so that a uniform material is left. The soil mixtures were prepared according to volume ratio, and their initial water content and water absorption were measured.

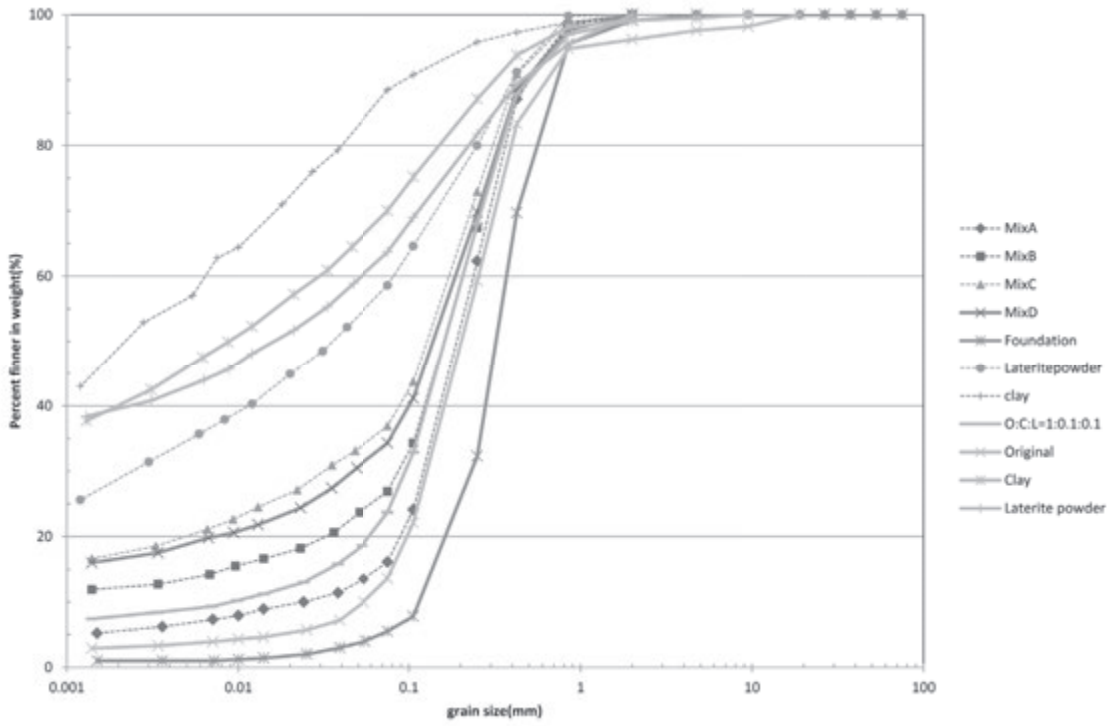

Fig. 13 : Consolidation of the coarse excavated sand by mixing clay

Using a rammer, the test soils were compacted from a spreading depth of 10cm to a compacted depth of 6cm. Then, after compacting the areas that come into contact with laterite, a Yamanaka hardness meter was used to control the degree of compaction. After confirming that the control conditions are satisfied, the soils were applied and compacted in sequence. Once the prescribed thickness was obtained, a simple penetration test, loading test, permeability test and density test were conducted to inspect the quality of the test foundation.

To verify the quality of the test foundation, a Yamanaka hardness test, simple penetration test, loading test, permeability test and local density test were performed immediately after completion of the test foundation and after roughly a month of curing. The erosion resistance of bare holes and side walls were also examined by pouring or sprinkling water.

Table 4 shows the result of the local density test. The dry density of the lower platform is 1.47g/cm^{3}as shown in Table 2, but as test soil A and test soil B of the test foundation had dry densities of 1.55g/cm^3 and 1.7g/cm^3, respectively, a considerable improvement in density was achieved particularly in test soil B.

Fig. 14 shows the result of the loading test. A limiting value could not be obtained due to a shortage of reaction force, but it was estimated from mutual similarity in a cone test. The result showed that an ultimate bearing capacity of more than 1500kN/m2 could be expected immediately after completion of the test foundation. This ultimate bearing capacity far exceeds the 900kN/m2 and more ultimate bearing capacity required by the foundation material of the South Temple, and verified that a large safety factor could be ensured even immediately after completion of the test foundation. Additionally, in the erosion resistance test performed by pouring and sprinkling water, no case of erosion was observed as that seen in a same test on the excavated soil, so erosion resistance was achieved.

	Test A		Test B	
	1	2	1	2
Wet density (g/cm3)	1.626	1.771	1.819	1.911
Water content (%)	9.80	8.69	9.71	9.53
Dry density (g/cm3)	1.481	1.630	1.658	1.745
Average dry density (g/cm3	1.555		1.701	

Table 4: Local density

Fig. 15 shows a test that was performed to verify the increase in strength of the test foundation, after roughly a month of curing. The consolidated soil contains slaked lime, so strength was expected to increase. This was confirmed in Fig. 14. The dashed lines represent N values immediately after completion of the test foundation, and the solid lines represent N values after a month of curing. From the relationship between N values and ultimate bearing capacities accumulated in restoration projects at the Angkor Monuments, the following formula has been obtained in regard to materials containing fine particles.

$$q_f = 150N \quad (kN/m^2)$$

When assuming an N value of 20 immediately after completion of the test foundation, an ultimate bearing capacity of approximately 3000kN/m2 can be expected. On the other hand, after a month of curing, the N value of test soil A was approximately 50, and that of soil B was approximately 250, so an increase was seen in the strength of the test foundation, although the values largely vary according to the mixing condition of the materials. Test soil A, which is a mixture of excavated soil and slaked lime, and test soil B, which is a mixture of excavated soil, clay, laterite powder and slaked lime, showed a roughly ten-fold increase in strength immediately after completion of the test foundation. The effectiveness of mixing clay and laterite powder is thus apparent.

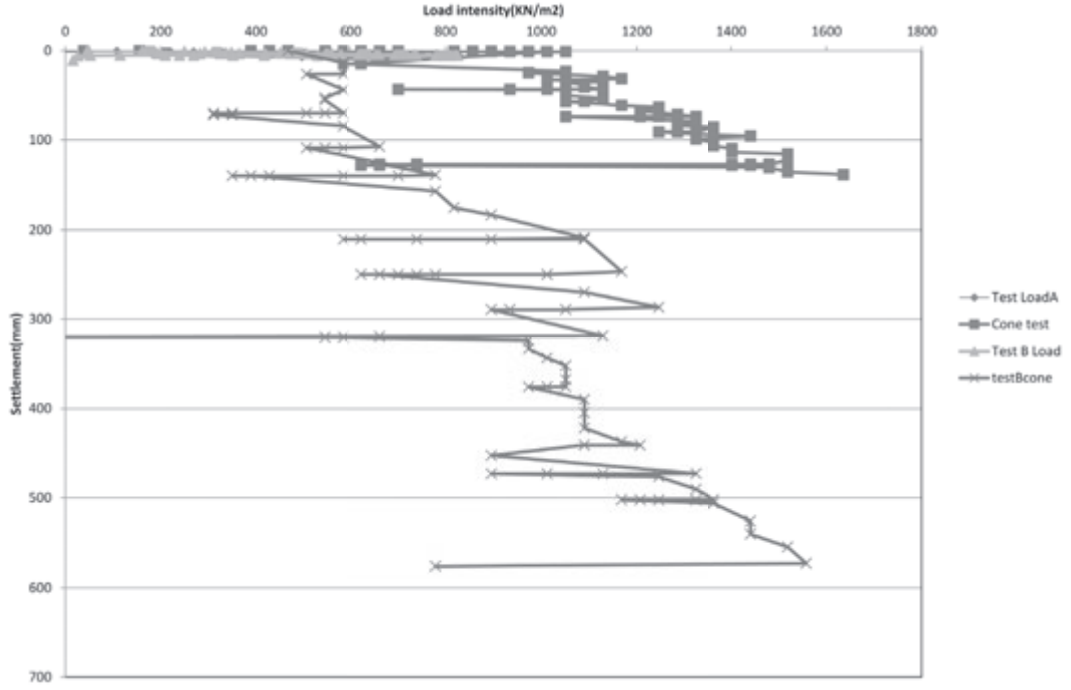

Fig. 14: Strength evaluation by loading test immediately after completion of the test foundation

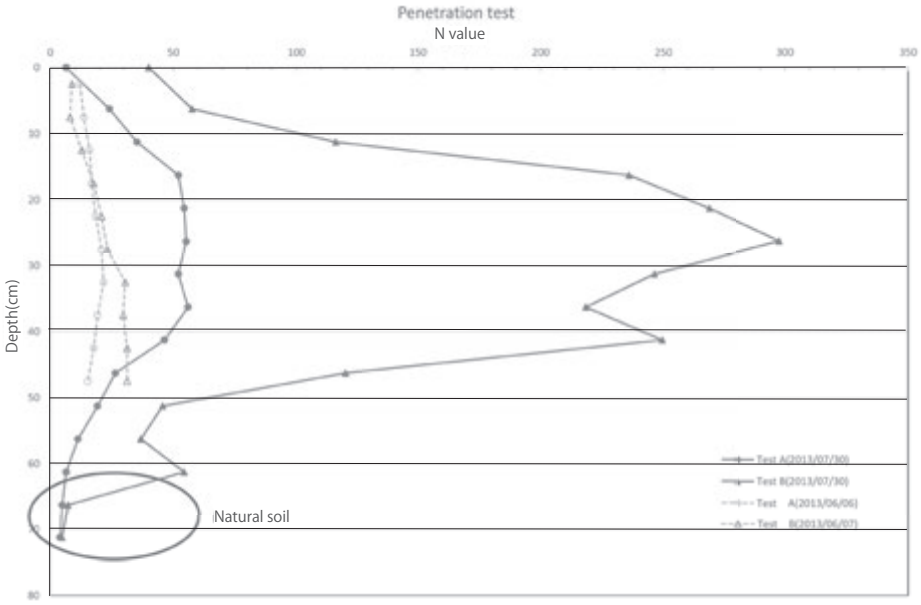

Fig. 15: Effectiveness after a month of curing

Photo 10: Removing foreign matter

Photo 11: Weighing the blended soil

Photo 12: Blending

Photo 13: Measuring the water content of a soil mixture

Photo 14: Adding water

Photo 15: Soil spreading thickness and compacted thickness

Photo 16: Leveling and compacting using a round rammer

Photo 17: Compacting using an "elephant's foot" rammer

Photo 18: Compacting the areas that come into contact with laterite

Photo 19: Compaction control using a Yamanaka hardness meter

Photo 20: Delamination prevention of the compacted soil surface

Photo 21: Quality inspection by a simple penetration test immediately after completion of the test foundation

Photo 22: Quality inspection by a loading test immediately after completion of the test foundation

Photo 23: Inspection of quality change by adding water

Photo 24: Adding water to a bare hole to see if it can keep its shape

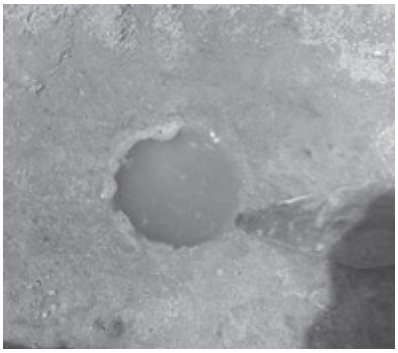

Photo 25: Strength test on the side walls after curing

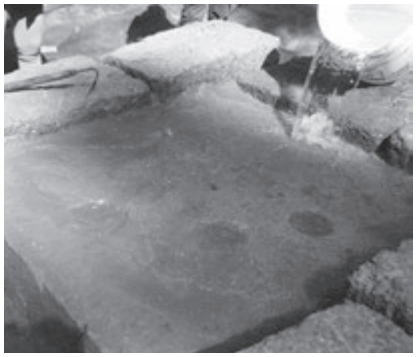

Photo 26: Water supply test after curing

Photo 27: Confirmation of erosion resistance and inspection of the side walls after curing

A	Requried load and deformation conditions	Unit	West top	Remarks
	Estimated maximum load intensity	kN/m^2	326	
	Requried bearing capacity	kN/m^2	978	Safety factor=3
	Allowabte settlement	mm	5	
	Coefficient of subgrade reaction	kN/m^3	195600	
B	Requried mixing conditions for compacted soil layers			
	Dry density(Pd)	g/cm^3	1.8	
	Water content of blended soil(W)	%	10	
	Mixing rate of dry weteht for base soil	%	100	
	Mixing rate of dry weight for laterite powder!	%	10	
	Mixine rate of dry weight for attended clay soil	%	10	
	Mixing rate of dry weight for slaked lime	%	20	Weight of blended soil=100
C	Compacting			
	Initial thickness	cm	10	
	compacted thickness	cm	6	
D	Requrted initial mechanical properties of compacted soil layers immidiatlv afetr compacted			
	Uniaxial strength	kN/m^2	978	
	Elastic deformation regidity	kN/m^2	258219.8	E_{50}=294.1(q_u-100)
	N value	blows	6.5	qf=150N
	YI(Yamanaka hardness inspctor)		25	
E	Estimated final properties after curing period of 90days			
	Uniaxial strength	kN/m^2	3292	qu=400+26(d-1)
	Elastic deformation rigidity	kN/m^2	938767.2	E_{50}=294.1 (q_u-1OO)
	Coefficient of subgrade reaction	kN/m^3	1304886.4	K =1.39/B*E_{50} (B=1m)
	Predicted settlement caused by weight of tower	mm	0.7	

Table 5: Soil control criteria

A test will be conducted on the test foundation once more immediately before commencing restoration work to examine the relationship between the foundation preparation method and control criteria as shown in Table 5.

7. Thorough Prevention of Foundation Material Runoff Using Geotextile

Deformation of the South Temple of West Prasat Top is assumed to be caused by the loose, coarse sand of the foundation. Thus, rather than using the coarse sand as it is, its strength and erosion resistance could be fully increased by mixing it with clay and laterite, treating it with slaked lime, and controlling it under the criteria shown in Table 4. However, to ensure safety, a nonwoven textile for runoff prevention will be applied to control runoff accompanying wastewater discharge from the foundation material. Fig. 16 shows an example of applying unwoven textile. In this case, the textile prevents clay from flowing into and clogging the drainage pipe accompanying the flow of external water into the drainage pipe.

In the case of the foundation of the South Temple of West Prasat Top, the unwoven textile would be placed along the side walls of the foundation to prevent the runoff of fine particles from inside the foundation. In consideration of the fact that groundwater level reaches the height of the lines of stones during the rainy season, and that such changes in groundwater level strengthens the soil below the line of stones, the unwoven textile would be laid on the bottom surface of the foundation as though to cover the stone lines. This would also convey to later generations that West Prasat Top was excavated down to this surface. The following are four general parameters for selecting an unwoven textile product.

1) Weight (g/m2)
2) Thickness (mm)
3) Coefficient of permeability in the vertical direction (cm/sec)
4) Apparent opening size (mm)

Opening size is determined by the grain size of the soil that is to be prevented from flowing in or out, and could be roughly defined as D85/Opening size of the textile > 1. D85 is the maximum diameter of 85% of the particles that pass through the textile in terms of the grain size distribution curve. With reference to Fig. 13, an opening diameter of roughly 0.2mm (200μm) can be obtained. A plastic board drain is also used in some cases for improvement of clayey ground. In this case, the core material is covered with unwoven textile to prevent clay particles from getting into the core material. The average opening diameter of this unwoven textile would be 50μm.

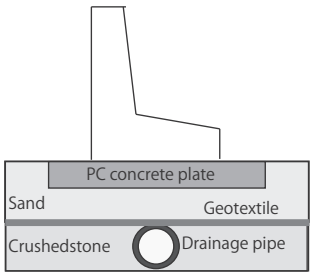

Fig. 16: Unwoven textile application example

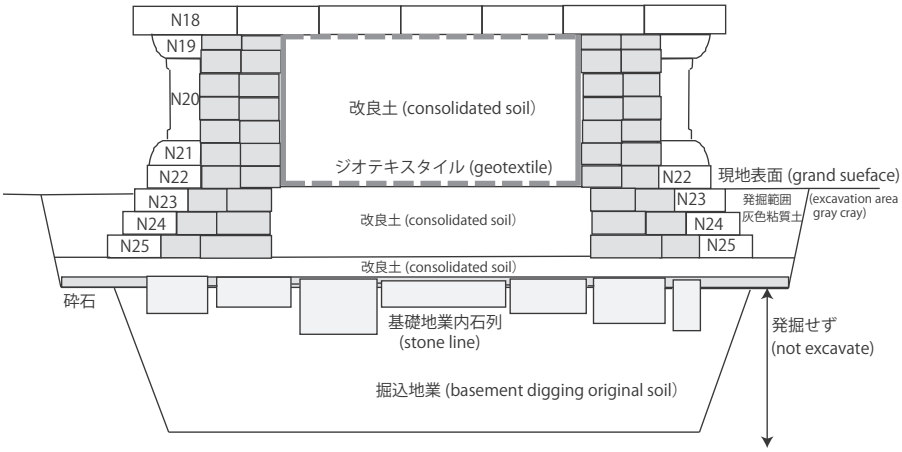

Fig. 17: Covering the foundation material with unwoven fabric